

AN OPTIMUM OPERATION OF A BULLDOZER  
RUNNING ON A WEAK TERRAIN

Tatsuro Muro

Prof., Department of Ocean Engineering  
Faculty of Engineering, Ehime University  
3 Bunkyo-cho, Matsuyama, Japan

ABSTRACT

Establishing an automatically controlled system to obtain a maximum productivity of a bulldozer running on a weak terrain, the total traffic performance of a tracked vehicle could be clarified by use of a micro-computer in robotics from initial informations of terrain material and vehicle dimensions. Here, an useful estimation method of terrain properties : cohesion, angle of internal friction, modulus of shear deformation, pressure sinkage curve at rest and slippage state was presented by use of input data from several sensors which could measure the initial sinkage of vehicle, and the torques and the slip sinkages for three slip ratios. Afterwards, an optimum drawbar-pull and an optimum slip ratio to get a maximum productivity in dozing operation of a small test bulldozer running on a weak remolded silty loam terrain could be determined from the relations between driving force, drawbar-pull, sinkage, eccentricity and slip ratio.

1. Introduction

To obtain a maximum effective rate of production of a bulldozer running on a weak terrain from the relation between drawbar-pull and slip ratio, it is necessary to estimate the locomotion resistance at driving state. The compaction resistance could be determined from the rut depth by use of the pressure sinkage curve of terrain material at rest and slippage state. On the other hand, the thrust of bulldozer could be calculated under the various distribution of contact pressure from the shear slippage curves which are expressed by the cohesion, the angle of internal friction and the modulus of shear deformation of terrain material, and the normal pressure. Then, the drawbar-pull of bulldozer could be determined under various slip ratios and eccentricities by means of the mechanical analyses of vehicle motion.

To establish an automatic control system to get an optimum operation of a bulldozer running on a weak terrain, an useful estimation method of those terrain properties from initial vehicle sinkages at rest, and torques, front and rear sinkages at 3 slippage states was presented. Those sinkages, torques and slip ratios should be measured directly by use of each sensor. Afterwards, both thrust slippage and drawbar-pull slippage curves could be automatically calculated by use of those terrain properties. The aim of an optimum operation of the bulldozer is to obtain a maximum effective rate of production.

Here, the optimum drawbar-pull and the slip ratio to get a maximum effective rate of production of a bulldozer model running on a weak silty loam were presented by use of a microcomputer.

## 2. Terrain conditions

### 2.1 Pressure sinkage curve

To estimate the static sinkage of track belt of a bulldozer on a weak terrain, several pressure sinkage curves of the soil are usually determined by means of plate loading tests as

$$\begin{aligned} p &= k s^n \\ &= (k_c/b + k_\phi) s^n \end{aligned} \quad (1)$$

where  $p$  is the normal contact pressure acting on the plate,  $s$  is the sinkage,  $b$  is the short side of the plate and  $k$ ,  $k_c$ ,  $k_\phi$  and  $n$  are the soil constants.

On the other hand, the soil constants  $k$  and  $n$  could be adversely determined from the static sinkage of frontidler  $S_{f0}$  and that of rear sprocket  $S_{r0}$  which might be directly measured by use of two sinkage sensors mounted on the bulldozer. The static normal contact pressure  $p_{f0}$  and  $p_{r0}$ , which acts under the frontidler and the rear sprocket respectively and the trim angle  $\theta_t$  could be calculated as

$$p_{f0} = (1 - 6e) W \cos \theta_t / 2BD \quad (2)$$

$$p_{r0} = (1 + 6e) W \cos \theta_t / 2BD \quad (3)$$

$$\theta_t = \sin^{-1} \left( \frac{S_{r0} - S_{f0}}{D} \right) \quad (4)$$

where  $W$  is the vehicle weight,  $B$  is the track width,  $D$  is the track length and  $e$  is the eccentricity of gravity center of the bulldozer.

Substituting those data into Eq.(1), the soil constants  $k$  and  $n$  could be calculated easily as

$$\begin{aligned} k &= p_{f0} / S_{f0}^n \quad \text{or} \quad p_{r0} / S_{r0}^n \\ n &= \log(p_{f0} / p_{r0}) / \log(S_{f0} / S_{r0}) \end{aligned} \quad (5)$$

, then the compaction resistance of the bulldozer running on a weak terrain will be estimated at driving state.

### 2.2 Shear slippage curve

The thrust of bulldozer which is developed at the bottom of track belt can be calculated from the relation between shear resistance  $\tau$  and amount of slippage  $j$  as shown in

$$\tau = (c + p \tan \phi) \{1 - \exp(-a j)\} \quad (6)$$

where  $p$  is the normal contact pressure,  $c$  is the cohesion,  $\phi$  is the angle of internal friction, and "a" is the modulus of shear deformation of soil. This shear slippage curve and the soil constants  $c$ ,  $\phi$  and "a" are usually determined by several traction tests for some track model plate.

Here, an estimation method of those soil constants of weak terrain is presented by use of the total thrusts, and the dynamic sinkages under the frontidler and rear sprocket which are measured directly at three slip ratios from a torque sensor mounted on the rear driving sprocket and the same sinkage sensor as mentioned previously.

Using the dynamic sinkages  $S_f$  and  $S_r$  measured at the frontidler and at the rear sprocket respectively, the trim angle  $\theta_{ti}$  could be determined as

$$\theta_{ti} = \sin^{-1} \left( \frac{S_r - S_f}{D} \right) \quad (7)$$

and the compaction resistance  $T_2$  could also be calculated. After determining the drawbar-pull  $T_4$  from the thrust  $T_3$ , the eccentricity  $e_i$  of resultant normal force  $P$  could be determined. Then, the normal contact pressure  $p$  acting under the bottom of track plate could be calculated

together with the amount of slippage  $j$  for the 3 kinds of slip ratios.

Integrating the shear resistance  $\tau$  in Eq.(6) along the track length, the total thrust  $T_3$  can be expressed in general as

$$T_3(N) = CC(N) \cdot c + CT(N) \cdot \tan\phi \quad (8)$$

where  $N=1, 2$  and  $3$ ,  $CC$  is the coefficient of cohesion  $c$  and  $CT$  is the coefficient of  $\tan\phi$ .

Therefore, the unknown value  $c$  and  $\tan\phi$  can be solved as

$$c = \frac{T_3(1)CT(2) - T_3(2)CT(1)}{CC(1)CT(2) - CC(2)CT(1)} \quad (9)$$

$$\tan\phi = \frac{T_3(1)CC(2) - T_3(2)CC(1)}{CT(1)CC(2) - CT(2)CC(1)} \quad (10)$$

where  $T_3(N)$  is given by use of the driving force  $T_1(N)$  measured directly from the torque sensor, assuming that the external driving torque equals the internal one subtracting a rolling resistance of road rollers, as

$$T_3(N) = W \sin\theta_{ti} + \frac{R_r}{R_r + H} T_1(N) \quad (11)$$

where  $R_r$  is the radius of rear sprocket and  $H$  is the grouser height.

Substituting the soil constants  $c$  and  $\tan\phi$  into Eq.(8), the theoretical total thrust  $T_3'(3)$  is able to calculate for another slip ratio.

$$\begin{aligned} E.F. &= T_3(3) - T_3'(3) \\ &= T_3(3) - \{CC(3) \cdot c + CT(3) \cdot \tan\phi\} \end{aligned} \quad (12)$$

The difference  $E.F.$  between the measured total thrust  $T_3(3)$  and  $T_3'(3)$  which is calculated for an assumed modulus of shear deformation of soil "a" could be reduced to zero by means of a two division method. As the result, the unknown value "a" is able to determine rapidly by use of a microcomputer.

### 3. Mechanical analyses of vehicle

#### 3.1 Thrust

The total thrust<sup>1)</sup> is developed not only on the straight part of bottom track belt but also on the parts of frontidler and rear sprocket, as shown in Fig.1.

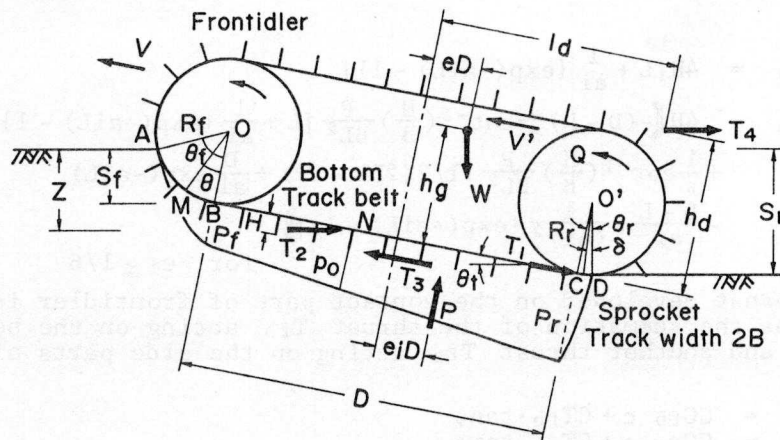


Fig.1 Several forces and dimensions of track belt at driving state

The thrust developed on the main parts of bottom track belt is expressed as the summation of the thrust  $T_{mb}$  acting on the bottom of grousers and the another thrust  $T_{ms}$  acting on the side parts of grousers as follows,

$$\begin{aligned} T_{mb} &= CC_{mb} \cdot c + CT_{mb} \cdot \tan \phi \\ T_{ms} &= CC_{ms} \cdot c + CT_{ms} \cdot \tan \phi \end{aligned} \quad (13)$$

where

$$\begin{aligned} CC_{mb} &= 2B \left[ D + \frac{1}{ai} \exp(-aj_B) \{ \exp(-aiD) - 1 \} \right] \\ CT_{mb} &= 2B \left\{ p_{fi} \left[ D + \frac{1}{ai} \exp(-aj_B) \{ \exp(-aiD) - 1 \} \right] + \frac{12e_i p_m}{D} \left[ \frac{D^2}{2} \right. \right. \\ &\quad \left. \left. + \frac{D}{ai} \exp\{-a(j_B + iD)\} + \frac{1}{(ai)^2} \exp(-aj_B) \{ \exp(-aiD) - 1 \} \right] \right\} \\ &\quad \text{for } |e_i| < 1/6 \\ i &: \text{slip ratio} \\ p_{fi} &: \text{normal contact pressure under frontidler at slip ratio } i \\ e_i &: \text{eccentricity of resultant normal force } P \\ p_m &: \text{average contact pressure} \\ j_B &: \text{amount of slippage at point } B \end{aligned}$$

and

$$\begin{aligned} CC_{mb} &= 2B \left[ L + \frac{1}{ai} \{ \exp(-aiL) - 1 \} \right] \\ CT_{mb} &= 2B \left\{ -\frac{P}{BL^2} (D - L) \left[ L + \frac{1}{ai} \{ \exp(-aiL) - 1 \} \right] + \frac{P}{BL^2} \left[ \frac{1}{2}(2DL - L^2) \right. \right. \\ &\quad \left. \left. + \frac{D}{ai} \exp(-aiL) - \frac{D-L}{ai} + \frac{1}{(ai)^2} \{ \exp(-aiL) - 1 \} \right] \right\} \\ L &= 3D(1/2 - e_i) \\ &\quad \text{for } e_i \geq 1/6. \end{aligned}$$

, and

$$\begin{aligned} CC_{ms} &= 4H \left[ D + \frac{1}{ai} \exp(-aj_B) \{ \exp(-aiD) - 1 \} \right] \\ CT_{ms} &= 4H \left\{ \frac{1}{\pi} p_{fi} \cot^{-1} \left( \frac{H}{B} \right) \left[ D + \frac{1}{ai} \exp(-aj_B) \{ \exp(-aiD) - 1 \} \right] \right. \\ &\quad \left. + \frac{12e_i p_m}{\pi D} \cot^{-1} \left( \frac{H}{B} \right) \left[ \frac{D^2}{2} + \frac{D}{ai} \exp\{-a(j_B + iD)\} \right. \right. \\ &\quad \left. \left. + \frac{1}{(ai)^2} \exp(-aj_B) \{ \exp(-aiD) - 1 \} \right] \right\} \\ &\quad \text{for } |e_i| < 1/6 \end{aligned}$$

and

$$\begin{aligned} CC_{ms} &= 4H \left[ L + \frac{1}{ai} \{ \exp(-aiL) - 1 \} \right] \\ CT_{ms} &= 4H \left\{ -(D - L) \frac{1}{\pi} \cot^{-1} \left( \frac{H}{B} \right) \frac{P}{BL^2} \left[ L + \frac{1}{ai} \{ \exp(-aiL) - 1 \} \right] \right. \\ &\quad \left. + \frac{1}{\pi} \cot^{-1} \left( \frac{H}{B} \right) \frac{P}{BL^2} \left[ \frac{1}{2}(2DL - L^2) + \frac{D}{ai} \exp(-aiL) \right. \right. \\ &\quad \left. \left. - \frac{D-L}{ai} + \frac{1}{(ai)^2} \{ \exp(-aiL) - 1 \} \right] \right\} \\ &\quad \text{for } e_i \geq 1/6 \end{aligned}$$

The thrust developed on the contact part of frontidler is also expressed as the summation of the thrust  $T_{fb}$  acting on the bottom of grousers and another thrust  $T_{fs}$  acting on the side parts of grousers as follows,

$$\begin{aligned} T_{fb} &= CC_{fb} \cdot c + CT_{fb} \cdot \tan \phi \\ T_{fs} &= CC_{fs} \cdot c + CT_{fs} \cdot \tan \phi \end{aligned} \quad (14)$$

where

$$\begin{aligned}
CC_{fb} &= 2BR_f \int_0^{\theta_f} [1 - \exp\{-aj_f(\theta)\}] \cos\theta \, d\theta \\
CT_{fb} &= 2BR_f \int_0^{\theta_f} \sigma_f(\theta) [1 - \exp\{-aj_f(\theta)\}] \cos\theta \, d\theta \\
j_f(\theta) &= R_f[(\theta_f - \theta) - (1 - i)\{\sin(\theta_f + \theta_{ti}) - \sin(\theta + \theta_{ti})\}] \\
\sigma_f(\theta) &= k[R_f\{\cos(\theta + \theta_{ti}) - \cos(\theta_f + \theta_{ti})\}]^n \times \cos(\theta + \theta_{ti}) \\
R_f &: \text{radius of frontidler} \\
\theta &: \angle \text{BOM} \\
\theta_f &: \text{entry angle}
\end{aligned}$$

and

$$\begin{aligned}
CC_{fs} &= 4HR_f \int_0^{\theta_f} [1 - \exp\{-aj_f(\theta)\}] \cos\theta \, d\theta \\
CT_{fs} &= 4HR_f \int_0^{\theta_f} \frac{1}{\pi} \sigma_f(\theta) \cot^{-1}\left(\frac{H}{B}\right) [1 - \exp\{-aj_f(\theta)\}] \cos\theta \, d\theta .
\end{aligned}$$

And the thrust developed on the contact part of rear sprocket also consists of the thrust  $T_{rb}$  acting on the bottom of grousers and another thrust  $T_{rs}$  acting on the side parts of grousers as follows,

$$\begin{aligned}
T_{rb} &= CC_{rb} \cdot c + CT_{rb} \cdot \tan\phi \\
T_{rs} &= CC_{rs} \cdot c + CT_{rs} \cdot \tan\phi
\end{aligned} \tag{15}$$

where

$$\begin{aligned}
CC_{rb} &= 2BR_r \int_0^{\theta_r} [1 - \exp\{-aj_r(\delta)\}] \cos(\theta_{ti} - \delta) \, d\delta \\
CT_{rb} &= 2BR_r \int_0^{\theta_r} \sigma_r(\delta) [1 - \exp\{-aj_r(\delta)\}] \cos(\theta_{ti} - \delta) \, d\delta \\
, \text{ and} \\
CC_{rs} &= 4HR_r \int_0^{\theta_r} [1 - \exp\{-aj_r(\delta)\}] \cos(\theta_{ti} - \delta) \, d\delta \\
CT_{rs} &= 4HR_r \int_0^{\theta_r} \frac{1}{\pi} \sigma_r(\delta) \cot^{-1}\left(\frac{H}{B}\right) [1 - \exp\{-aj_r(\delta)\}] \cos(\theta_{ti} - \delta) \, d\delta . \\
j_r(\delta) &= R_r\{(\theta_{ti} - \delta) - (1 - i)(\sin\theta_{ti} - \sin\delta)\} + iD + j_B \\
\sigma_r(\delta) &= k[R_r\{\cos\theta_{ti} - \cos(\theta_{ti} - \delta)\} + D \sin\theta_{ti} + R_r(\cos\delta - \cos\theta_{ti})]^n \\
&\quad \times \cos\delta \\
\delta &: \angle \text{DO}'C \\
\theta_r &: \text{exit angle}
\end{aligned}$$

$$\text{for } |e_i| < 1/6$$

and

$$\begin{aligned}
j_r(\delta) &= R_r\{(\theta_{ti} - \delta) - (1 - i)(\sin\theta_{ti} - \sin\delta)\} + iL \\
\sigma_r(\delta) &= k\{L \sin\theta_{ti} + R_r(\cos\delta - \cos\theta_{ti})\}^n \times \cos\delta \\
&\quad \text{for } e_i \geq 1/6 .
\end{aligned}$$

Then, the total thrust  $T_3$  is obtained as the summation of each thrust by

$$T_3 = T_{mb} + T_{ms} + T_{fb} + T_{fs} + T_{rb} + T_{rs} \tag{16}$$

and

$$\begin{aligned}
CC &= CC_{mb} + CC_{ms} + CC_{fb} + CC_{fs} + CC_{rb} + CC_{rs} \\
CT &= CT_{mb} + CT_{ms} + CT_{fb} + CT_{fs} + CT_{rb} + CT_{rs} .
\end{aligned}$$

For  $e_i \geq 1/6$ ,  $T_{fb} = T_{fs} = 0$ ,  $CC_{fb} = CC_{fs} = 0$  and  $CT_{fb} = CT_{fs} = 0$ .

### 3.2 Compaction resistance

The sinkage of track belt under the frontidler  $S_f$  and that under the rear sprocket  $S_r$  of a bulldozer running on a weak terrain can be expressed generally by

$$\begin{aligned}
S_f &= S_{f0} \\
S_r &= S_{r0} + S_{ri}
\end{aligned} \tag{17}$$

where  $S_{ri}$  is the slip sinkage at the rear sprocket at slip ratio  $i$ .

For trapezoidal distribution of contact pressure,  $S_{f0}$  and  $S_{r0}$  can be

calculated from the front contact pressure  $p_{fi}$  and the rear one  $p_{ri}$  respectively. But, for triangular one,  $S_f$  can be obtained as

$$S_f = S_r(1 - D/L) < 0. \quad (18)$$

By the way, the slip sinkage  $S_s$  was expressed by M.G.Bekker<sup>2)</sup> as

$$S_s = \frac{k'(p - p_0)}{c + p \tan \phi} \cdot j \quad (19)$$

where  $p_0$  is the critical bearing capacity of the weak terrain.

For trapezoidal distribution of contact pressure i.e.  $|e_i| < 1/6$ , the total slip sinkage  $S_{ri}$  is calculated by

$$S_{ri} = \frac{k' i V'}{\tan \phi} \left\{ -\left(p_0 + \frac{c}{\tan \phi}\right) \frac{D}{12 p_{mei} (1-i) V'} \times \log \frac{t_D + b'}{t_N + b'} + t_D - t_N \right\} \cos \theta_{ti}$$

where

$$\begin{aligned} t_D &= \frac{1}{1-i} \frac{D}{V'} \\ t_N &= \frac{p_0 - p_m(1-6e_i)}{12 e_i p_m} \frac{1}{1-i} \frac{D}{V'} \\ b' &= \frac{c + p_f \tan \phi}{\tan \phi} \frac{D}{12 p_{mei} (1-i) V'} \end{aligned} \quad (20)$$

$V'$  : speed of track belt

assuming that any slip sinkage does not occur within the contact pressure  $p_0$ .

For triangular distribution of contact pressure i.e.  $e_i \geq 1/6$ , the total slip sinkage  $S_{ri}$  is calculated by

$$S_{ri} = \frac{k' i V'}{\tan \phi} \left\{ -\left(p_0 + \frac{c}{\tan \phi}\right) \frac{BL^2}{P(1-i) V'} \times \log \frac{t_D + f}{t_Y + f} + t_D - t_Y \right\} \cos \theta_{ti}$$

where

$$\begin{aligned} t_D &= \frac{1}{1-i} \frac{L}{V'} \\ t_Y &= \frac{1}{1-i} \frac{L}{V'} \frac{p_0 BL}{P} \\ f &= \frac{c}{\tan \phi} \frac{BL^2}{P(1-i) V'} \end{aligned} \quad (21)$$

Therefore, the compaction resistance  $T_{2i}$  can be calculated by

$$T_{2i} = \frac{2kB}{n+1} \cdot S_{ri}^{n+1}. \quad (22)$$

### 3.3 Drawbar-pull

The force balances between  $W$ ,  $T_2$ ,  $T_3$ ,  $T_4$  and  $P$  are given by

$$T_2 + T_4 = T_3 \cos \theta_{ti} - P \sin \theta_{ti} \quad (23)$$

$$W = P \cos \theta_{ti} + T_3 \sin \theta_{ti}. \quad (24)$$

Therefore

$$P = W \cos \theta_{ti} - (T_2 + T_4) \sin \theta_{ti} \quad (25)$$

is obtained.

The eccentricity  $e_i$  can be calculated from the balance of moment around the axis of rear sprocket as follows,

$$e_i = \frac{1}{2} + \frac{1}{PD} [-T_2(R_r - S_r + Z) + T_4 \{h_d \cos \theta_{ti} - (l_d - D/2) \sin \theta_{ti} - R_r \cos \theta_{ti}\} + W(h_g + H) \times \sin \theta_{ti} - WD(1/2 - e) \cos \theta_{ti}] \quad (26)$$

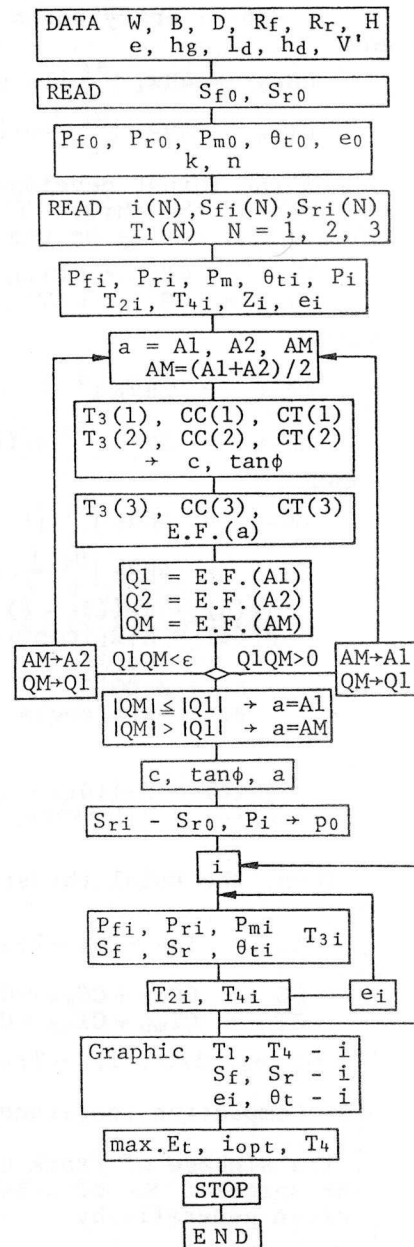


Fig.2 Flow chart for an optimum operation of bulldozer

where  $Z$  is the depth of point on which  $T_2$  acts horizontally,  $h_d$  is the height of point applying drawbar-pull,  $l_d$  is the distance between vehicle central axis and the point applying drawbar-pull,  $h_g$  is the height of vehicle gravity center and  $e$  is the eccentricity of gravity center of bulldozer. Therefore, the drawbar-pull  $T_4$  can be determined as

$$T_4 = \frac{T_3}{\cos\theta_{ti}} - W \tan\theta_{ti} - T_2 \quad (27)$$

#### 4. Microcomputer

##### 4.1 Flow chart

Fig.2 shows the flow chart for determining the soil constants and for calculating the traffic performance of bulldozer running on a weak terrain to obtain an optimum operation. In the beginning, several initial data ;  $W, B, D, R_f, R_r, H, e, h_g, h_d, l_d$ , and speed of track belt  $V'$  are given. To determine the soil constants  $k$  and  $n$  of pressure sinkage curve of the terrain, and the initial contact pressures  $p_{f0}, p_{r0}, p_{m0}$ , the initial trim angle  $\theta_{t0}$  and the initial eccentricity  $e_0$ , the initial sinkage of frontidler  $S_{f0}$  and that of rear sprocket  $S_{r0}$  at rest stage of bulldozer on the weak terrain should be taken into the microcomputer from the sinkage sensors. And then the slip ratios  $i(N)$ , the sinkages  $S_{fi}(N), S_{ri}(N)$  and the driving force  $T_1(N)$  for  $N=1, 2$  and  $3$  at three slippage stages should be taken into the microcomputer from the sinkage and torque sensors to calculate the contact pressures  $p_{fi}, p_{ri}, p_{mi}$ , the trim angle  $\theta_{ti}$ , the resultant normal force  $P_i$ , the compaction resistance  $T_{2i}$ , the drawbar-pull  $T_{4i}$ , the depth acting compaction resistance  $Z_i$  and the eccentricity  $e_i$  at each slippage stage. For determining the soil constants  $c, \tan\phi$  and "a", the two division method is used for the error function Eq.(12). Also, the unknown value  $p_0$  can be determined from the error function between the measured amount of slip sinkage and the theoretical one given in Eq.(20) or (21) by means of the two division method.

Afterwards, the contact pressure  $p_{fi}, p_{ri}$  and  $p_{mi}$ , the sinkage  $s_{f0}, s_{r0}$  and the slip sinkage of rear sprocket  $s_{ri}$ , the trim angle  $\theta_{ti}, T_{3i}, T_{2i}$  and  $T_{4i}$  can be calculated for any slip ratio  $i$  from zero to 100%. Those values are repeatedly calculated for both trapezoidal and triangular distribution of contact pressure until the eccentricity  $e_i$  is determined. And then, the optimum slip ratio  $i_{opt}$  to obtain the maximum traffic efficiency of power  $\max.E_t$  and the optimum slip ratio  $i_{opt}$  to obtain the maximum productivity  $\max.Q$  can be determined immediately, by use of  $T_1 - i$  curve and  $T_4 - i$  curve.

##### 4.2 Driving force, drawbar-pull and slippage

For an example, the relations between

Table 1 Dimensions of test vehicle

Weight of vehicle	$W$	3.55 kN
Width of track belt	$B$	20.0 cm
Contact length of track belt	$D$	71.0 cm
Interval of central axes of 2 track belts	$L_c$	67.2 cm
Radius of front-idler	$R_f$	14.8 cm
Radius of rear sprocket	$R_r$	14.8 cm
Height of grouser	$H$	3.2 cm
Grouser pitch	$G_p$	20.4 cm
Eccentricity	$e$	- 0.010
Height of gravity center of vehicle	$h_g$	35.3 cm
Distance between central axis of vehicle and point acting drawbar-pull	$l_d$	50.8 cm
Height of point acting drawbar-pull	$h_d$	32.5 cm
Speed of track belt against vehicle	$V'$	9.4 cm/s

$T_4$ ,  $T_1$  and  $i$  have been measured experimentally for a small test vehicle running on a weak remolded silty loam terrain. Table 1 shows the dimensions of test vehicle and track belt. The track belt has 22 standard T type grousers of which height  $H$  is 3.2 cm and grouser pitch  $G_p$  is 20.4 cm. The driving force  $T_1$  of the test vehicle mounted 1.5 kW electric motor have been directly measured by use of torque sensor. And the drawbar-pull  $T_4$  have been directly measured by use of a load cell which has been connected with a drawing wire rope wound by 3.7 kW electric motor at a given speed of traction. And the initial and slip sinkage of front-idler  $s_{f0}$ ,  $s_{fi}$  and those of rear sprocket  $s_{r0}$ ,  $s_{ri}$  have been measured by use of slip sinkage sensors. Table 2 shows the physical soil properties of the remolded silty loam. Photo.1 shows the test vehicle having rigid track belt under traction at slip ratio 44%. Fig.3 shows the experimental results of  $T_1$ ,  $T_4$  and  $i$  relationship. Both forces  $T_1$  and  $T_4$  tend to increase with the increment of slip ratio, and also the locomotion resistance

Table 2 Physical soil properties of silty loam

Specific gravity	$G_s$	2.84
Liquid limit	L.L	33.2 %
Plastic limit	P.L	21.4 %
Plasticity index	$I_p$	11.8 %
Grain size distribution	Coefficient of uniformity $U_c$	6.40
	Coefficient of curvature $C_c$	0.31
	Average grain size $D_{50}$	54 $\mu$ m
Unit weight	$\gamma_t$	18.2 kN/m <sup>3</sup>
Void ratio	$e$	0.85
Water content	$W$	30.0 %

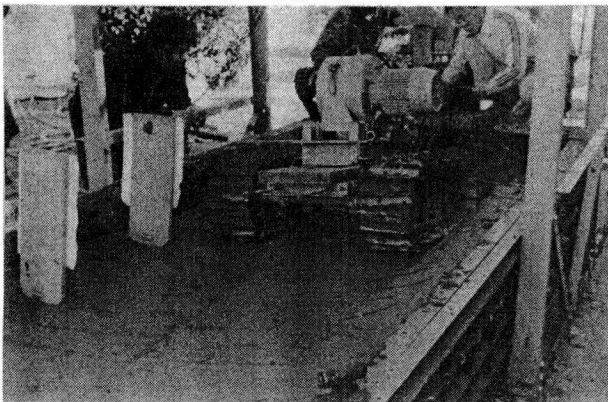


Photo.1 Test vehicle running at  $i = 44\%$

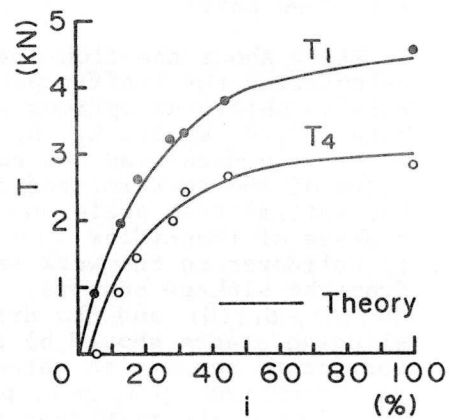


Fig.3 Relations between driving force  $T_1$ , drawbar-pull  $T_4$  and slip ratio  $i$   
 $T_1 = (1 + H/R_r)(T_3 - W \sin \theta_t)$

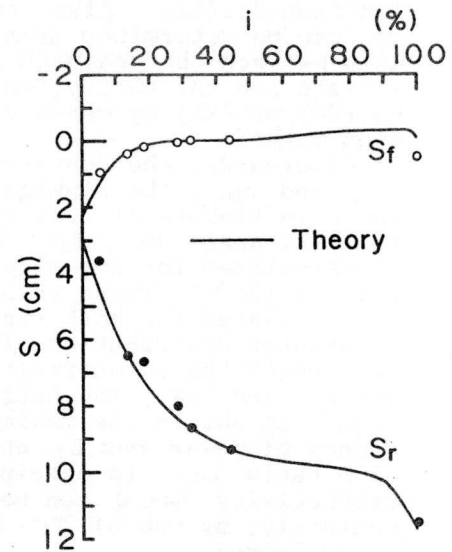


Fig.4 Relations between sinkage of frontidler  $S_f$ , sinkage of rear sprocket  $S_r$  and slip ratio  $i$

which is expressed as the difference between  $T_1$  and  $T_4$  on the whole tends to increase with the increment of slip ratio. Fig.4 shows the experimental data of the sinkage  $S_f$ ,  $S_r$  and  $i$  relationship. The sinkage  $S_r$  increases remarkably due to slip sinkage with the increment of slip ratio as compared with the sinkage  $S_f$ .

Now, the initial sinkages  $sf_0$ ,  $sr_0$  at rest stage, and  $T_1(N)$ ,  $i(N)$  and  $S_{fi}(N)$ ,  $S_{ri}(N)$  at three slippage stages ( $N=1, 2$  and  $3$ ) which have been selected as input data are shown in Table 3, with the analytical results, the soil constants:  $c$ ,  $\tan\phi$  and "a",  $k$  and  $n$ , and the critical bearing capacity  $p_0$ .

The analytical relations between driving force, drawbar-pull and slip ratio, and the relations between front and rear sinkages and slip ratio are shown in the previous figure 3 and 4, respectively. And the theoretical variations of trim angle  $\theta_{ti}$  and eccentricity  $e_i$  with slip ratio are shown in Fig.5. Those analytical results agree fairly well with the experimental data.

#### 4.3 Automatic control system

The traffic efficiency of power  $E_t$  can be defined as

$$E_t = \frac{V T_4}{V' T_1} \times \left(1 + \frac{H}{R_r}\right) \cos\theta_t$$

$$= (1 - i) \frac{T_4}{T_1} \times \left(1 + \frac{H}{R_r}\right) \cos\theta_t \quad (28).$$

In this case, the maximum traffic efficiency of power could be obtained to be  $\max.E_t = 73.0\%$  for the optimum slip ratio  $i_{opt} = 4\%$  at  $T_{1opt} = 0.888 \text{ kN}$  and  $T_{4opt} = 0.556 \text{ kN}$ .

Furthermore, the maximum productivity  $\max.Q$  of the bulldozing operation which is given to be proportional to the maximum traffic power as

$$\max.Q = k_p V T_{4opt} \left(1 + \frac{H}{R_r}\right) \cos\theta_{ti}$$

$$= k_p (1 - i_{opt}) V' T_{4opt} \left(1 + \frac{H}{R_r}\right) \cos\theta_{ti} \quad (29)$$

is obtained at  $i_{opt} = 33\%$ ,  $T_{4opt} = 2.283 \text{ kN}$  and the maximum traffic power  $17.35 \text{ kNcm/s}$ .

To operate the bulldozer at this optimum slip ratio, the slip ratio  $i$ ,  $T_1$  or  $T_4$  should be controlled within the allowable range. For an example,  $T_4$  can be controlled by adjusting the vertical position of blade by use of some limit sensor as

$$T_4 = (1 \pm 0.2) T_{4opt} \quad (30)$$

considering that the bulldozer is engaged in a bulldozing operation.

#### 5. Conclusions

Table 3 Input data and calculated soil constants

$S_{f0} = 3.66 \text{ cm}$ $S_{r0} = 1.91 \text{ cm}$	$k = 0.0827$ $n = 0.435$
$i(1) = 0.13$ $S_{fi}(1) = 0.43 \text{ cm}$ $S_{ri}(1) = 6.51 \text{ cm}$ $T_1(1) = 1.96 \text{ kN}$	$c = 7.94 \text{ kPa}$ $\tan\phi = 0.459$
$i(2) = 0.32$ $S_{fi}(2) = 0.03 \text{ cm}$ $S_{ri}(2) = 8.69 \text{ cm}$ $T_1(2) = 3.32 \text{ kN}$	$a = 0.101$ $p_0 = 6.86 \text{ kPa}$
$i(3) = 0.44$ $S_{fi}(3) = 0.00 \text{ cm}$ $S_{ri}(3) = 9.30 \text{ cm}$ $T_1(3) = 3.78 \text{ kN}$	$k' = 0.005$

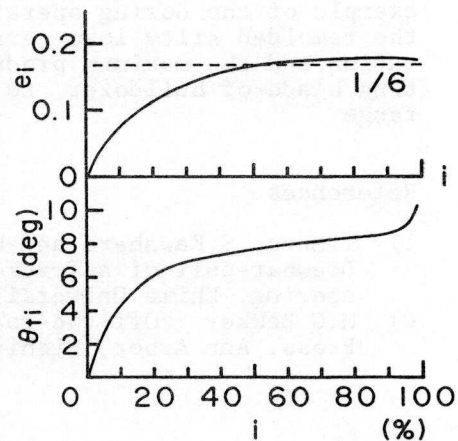


Fig.5 Variations of trim angle  $\theta_{ti}$  and eccentricity  $e_i$  with slip ratio  $i$

To obtain the optimum operation of a bulldozer running on a weak terrain, the optimum slip ratio should be determined to get the maximum traffic efficiency of power and the maximum productivity. Considering the relations between the driving force, the drawbar-pull and the slip ratio, it is necessary to estimate exactly the compaction resistance due to the rut depth of rear sprocket.

To develop an automatically controlled system, the terrain properties: cohesion, angle of internal friction, modulus of shear deformation, pressure sinkage curve and critical bearing capacity could be determined in the beginning from the initial sinkage of vehicle at rest state, the front and rear sinkages of vehicle and the driving torques at three slippage states which were measured directly from each sensor. Then the thrust developed under the track belt and the compaction resistance could be calculated from the shear slippage curve and the slip sinkage curve respectively. As the results, the relations between the driving force, the drawbar-pull, the vehicle sinkage and the eccentricity and the slip ratio could be rapidly determined from those terrain properties by use of the microcomputer simulation model TTM-2.

Afterwards, the optimum drawbar-pull and the optimum slip ratio to obtain the maximum productivity could be automatically determined for an example of the dozing operation of the small test bulldozer running on the remolded silty loam terrain. And also, the reasonable depth of excavation and the maximum productivity could be determined for the excavating blade of bulldozer, to control the drawbar-pull within the optimum range.

#### References

- 1) T.Muro, S.Kawahara and K.Omoto : Energy Analysis for an Effective Drawbar-pull of a Tracked Vehicle, Memoirs of the Faculty of Engineering, Ehime University, pp. 409 - 419 , Feb., 1988.
- 2) M.G.Bekker : Off-the-road locomotion, The University of Michigan Press, Ann Arbor, Michigan, pp. 113 - 147 , 1960.